

## Search for High Reactivity and Low Selectivity of Radicals toward Double Bonds: The Case of a Tetrazole-Derived Thiyl Radical

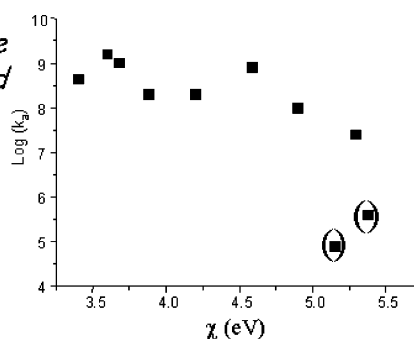
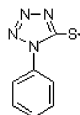
Jacques Lalevée,\* Xavier Allonas, and Jean Pierre Fouassier

Department of Photochemistry, Ecole Nationale Supérieure de Chimie de Mulhouse, 3 rue Alfred Werner, 68093 Mulhouse Cedex, France

j.lalevee@uha.fr

Received August 30, 2006

Highly reactive  
tetrazole derived  
thiyl radical:



The search for new radical structures having both low selectivity and high reactivity toward the addition reaction onto alkenes can be of interest in organic synthesis or polymer chemistry and has led us to propose a new tetrazole-derived thiyl radical. The reactivity of this sulfur-centered structure is compared to that of an aminoalkyl radical also efficient for alkene addition. Worthwhile results are obtained; the new structure is more reactive on the complete range of alkenes with addition rate constants higher than  $10^7 \text{ M}^{-1} \text{ s}^{-1}$  for both electron-deficient (acrylonitrile, ...) or electron-rich (vinylether, ...) double bonds. Quantum mechanical calculations have allowed a better understanding of this unique feature.

### Introduction

The addition reaction of a radical to a double bond is usually depicted by a state correlation diagram (SCD),<sup>1–5</sup> which shows the potential energy profiles of the four lowest doublet configurations of the system consisting of the radical unpaired electron and the attacked  $\pi$ -bond electron pair (the reactant ground state, the reactant excited state, and two charge-transfer configurations CTC  $\text{R}^+/\text{DB}^-$  and  $\text{R}^-/\text{DB}^+$ ). The barrier obviously decreases upon increase of the exothermicity. The involvement of the polar effects can also greatly influence the reaction through a decrease of the barrier when decreasing the CTC energies.<sup>1,4–8</sup> This has been recently exemplified in the study of the reactivity of a large class of carbon-centered radicals

( $\text{C}^\bullet$ ) (including aminoalkyl radicals)<sup>6–8</sup> toward different alkenes: a clear separation and a quantification of both polar and enthalpy factors were proposed. The reactivity of sulfur-centered radicals ( $\text{S}^\bullet$ ) has clearly deserved much less attention than the reactivity of  $\text{C}^\bullet$ .<sup>1,9–12</sup> The investigated  $\text{C}^\bullet$  are known to usually exhibit a high selectivity toward double bonds;<sup>1</sup>  $\text{S}^\bullet$  are usually assumed to be less reactive toward double bonds than  $\text{C}^\bullet$  and their selectivity remains unclear.<sup>10–11</sup>

The search for new radical structures having both low

(1) Fischer, H.; Radom, L. *Angew. Chem., Int. Ed.* **2001**, *40*, 1340–1371.

(2) Heberger, K.; Lopata, A. *J. Org. Chem.* **1998**, *63*, 8646–8653.

(3) Shaik, S. S.; Shurki, A. *Angew. Chem., Int. Ed.* **1999**, *38*, 586–625.

(4) Shaik, S. S.; Canadell, E. *J. Am. Chem. Soc.* **1990**, *112*, 1446–1452.

(5) Wong, M. W.; Pross, A.; Radom, L. *J. Am. Chem. Soc.* **1994**, *116*, 6284–6292.

(6) Lalevée, J.; Allonas, X.; Fouassier, J. P. *J. Phys. Chem. A* **2004**, *108*, 4326–4334.

(7) Lalevée, J.; Allonas, X.; Fouassier, J. P. *J. Am. Chem. Soc.* **2003**, *125*, 9377–9380.

(8) Lalevée, J.; Allonas, X.; Fouassier, J. P. *J. Org. Chem.* **2005**, *70*, 814–819. Lalevée, J.; Allonas, X.; Fouassier, J. P. *Macromolecules* **2005**, *38*, 4521–4524.

(9) Tedder, J. M. *Angew. Chem., Int. Ed. Engl.* **1982**, *21*, 401–432.

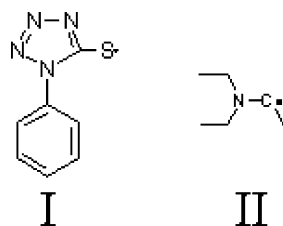
(10) Ito, O.; Nogami, K.; Matsuda, M. *J. Phys. Chem.* **1981**, *85*, 1365–1368.

(11) (a) Alam, M. M.; Konami, H.; Watanabe, A.; Ito, O. *J. Chem. Soc., Perkin Trans.* **1995**, *2*, 263–268. (b) Ito, O.; Tamura, S.; Matsuda, M.; Kenkichi, M. *J. Polym. Sci.: Part A: Polym. Chem.* **1987**, *26*, 1429–1438.

(12) Lalevée, J.; Allonas, X.; Morlet-Savary, F.; Fouassier, J. P. *J. Phys. Chem. A* **2006**, *110*, 11605–11612.

(13) Lalevée, J.; Allonas, X.; Fouassier, J. P. *J. Am. Chem. Soc.* **2002**, *124*, 9613–9621.

## SCHEME 1



selectivity and high reactivity relevant to organic synthesis or polymer chemistry has led us to propose the tetrazole-derived thiyl radical **I** (Scheme 1).

In this paper, the reactivity of **I** toward ten alkenes, chosen among monomers (vinyl ethyl ether, VE; vinyl acetate, VA; methyl acrylate, MA; acrylonitrile, AN; allyl butyl ether, ABE; acrylamide, AAM; N-vinylpyrrolidone, NVP; dimethyl fumarate, FU; dimethyl maleate, MAL; vinylcarbazole, VC) will be studied using laser flash photolysis and quantum mechanical calculations. Double bonds having very different electron acceptor/donor properties, strong enthalpy/polar effects on the addition reactions are thus expected. We will outline the low selectivity and the high reactivity of **I** toward both electrophilic and nucleophilic alkenes. This study will offer a good opportunity to separate the relative contributions of the polar and enthalpy effects in **I** and **II** and explain this unique feature of **I**.

## Experimental Section

The chemical compounds used were selected with the best purity available (5,5'-dithiobis(1-phenyl-1H-tetrazole, *tert*-butylperoxide). Triethylamine was purified by distillation. In the case of liquid monomers, the stabilizer (hydroquinone-methyl ether, HQME) was removed by column purification (AL-154). Vinylcarbazole was purified by recrystallization.

## Results

**Experimental Addition Rate Constants.** The tetrazole-derived thiyl radical **I** was generated from the photodissociation of the corresponding disulfide (5,5'-dithiobis(1-phenyl-1H-tetrazole) under laser irradiation at 355 nm. The corresponding radical **I** spectrum is centered at about 430 nm in agreement with previous studies.<sup>14</sup> The S–S bond cleavage occurs within the risetime of our experimental setup (<10 ns). The reaction used here for the observation of the aminoalkyl radical **II** consists of two consecutive steps as already proposed.<sup>15,16</sup> The first step is the generation of a *tert*-butoxyl radical through the photochemical decomposition of *tert*-butylperoxide; the second step corresponds to an  $\alpha$ (C–H) hydrogen abstraction reaction from triethylamine. Radical **II** is observed at 340 nm.

The addition rate constants to the different alkenes were determined by nanosecond laser flash photolysis (using the equipment described in ref 13; resolution time, 10 ns) from a classical Stern–Volmer analysis. To determine the addition and fragmentation rate constants ( $k_a$  and  $k_{-a}$ ) and the equilibrium constant ( $K = k_a/k_{-a}$ ) of **I**, we used the selective radical trapping flash photolysis method proposed in the literature.<sup>10–12</sup> For **II**,

**TABLE 1.** Rate Constants  $k_a$  of the Addition Reactions of **I** and **II** to Different Alkenes and Equilibrium Constant  $K$  of the Addition/Fragmentation Reactions of **I**

alkene	<b>I</b> <sup>a</sup>		<b>II</b> <sup>a</sup>
	$k_a$ (M <sup>-1</sup> s <sup>-1</sup> )	$K$ (M <sup>-1</sup> ) <sup>b</sup>	$k_a$ (M <sup>-1</sup> s <sup>-1</sup> )
AN	$2.5 \times 10^7$	33.3	$6.0 \times 10^7$
MA	$1.0 \times 10^8$	16.7	$3.0 \times 10^7$
VA	$2.0 \times 10^8$	4.17	$<5 \times 10^4$
VE	$4.4 \times 10^8$	16.7	$<5 \times 10^4$
ABE	$2.4 \times 10^8$	2.56	$<5 \times 10^4$
AAM	$8 \times 10^8$	16.7	$6.0 \times 10^6$
NVP	$1 \times 10^9$	25.6	$<5 \times 10^4$
VC	$1.9 \times 10^9$	37	$<5 \times 10^4$
FU	$4.5 \times 10^5$		$4.1 \times 10^8$
MAL	$8 \times 10^4$		$8.1 \times 10^7$

<sup>a</sup> The errors for the addition rate constants can be estimated to 5–10%.

<sup>b</sup> Using a  $k_{02}$  value of  $3 \times 10^9$  M<sup>-1</sup> s<sup>-1</sup> (ref 28).

the reaction is found to be irreversible. The addition rate constants of **I** and **II** as well as the equilibrium constants for the addition/fragmentation reactions of **I** are presented in Table 1.

**Quantum Mechanical Calculations.** For a better characterization of **I** and **II** reactivity, quantum mechanical calculations were carried out. The computational procedure has been already discussed in detail.<sup>6–8</sup> All of the calculations were performed using the hybrid functional B3LYP from the G98 or G03 program suites.<sup>17,18</sup> Reactants, products, and transition states (TS) were fully optimized, allowing the determination of the reaction enthalpy ( $\Delta H_R$ ), the amount of charge  $\delta^{\text{TS}}$  transferred from the radical to the alkene in the transition state structure, and the barrier. The barrier corresponds to the energetic difference between the TS and the reactants with the addition of the zero point energy correction. The activation energy ( $E_a^{\text{TS}}$ ) for the addition was obtained from the calculated barrier with the usual addition of the  $RT$  term.<sup>12,19,20</sup> The addition rate constants were also calculated; determination of the preexponential factor in the Arrhenius equation was made by the activated complex theory:<sup>19,20</sup> the harmonic oscillator approximation<sup>18–20</sup> was adopted for the activation entropy calculations. This approach was assumed accurate enough for our purposes.<sup>21</sup>

Adiabatic ionization potentials (IP) and adiabatic electron affinities (EA) characterizing the reactants were calculated by the previously used procedure (Table 2).<sup>6–8</sup> The electron-deficient or electron-rich character of the different alkenes is represented by their absolute electronegativity ( $\chi$ ) calculated

(17) Frisch, M. J.; Trucks, G. W.; Schlegel, H. B.; Scuseria, G. E.; Robb, M. A.; Cheeseman, J. R.; Zakrzewski, V. G.; Montgomery, J. A., Jr.; Stratmann, R. E.; Burant, J. C.; Dapprich, S.; Millam, J. M.; Daniels, A. D.; Kudin, K. N.; Strain, M. C.; Farkas, O.; Tomasi, J.; Barone, V.; Cossi, M.; Cammi, R.; Mennucci, B.; Pomelli, C.; Adamo, C.; Clifford, S.; Ochterski, J.; Petersson, G. A.; Ayala, P. Y.; Cui, Q.; Morokuma, K.; Salvador, P.; Dannenberg, J. J.; Malick, D. K.; Rabuck, A. D.; Raghavachari, K.; Foresman, J. B.; Cioslowski, J.; Ortiz, J. V.; Baboul, A. G.; Stefanov, B. B.; Liu, G.; Liashenko, A.; Piskorz, P.; Komaromi, I.; Gomperts, R.; Martin, R. L.; Fox, D. J.; Keith, T.; Al-Laham, M. A.; Peng, C. Y.; Nanayakkara, A.; Challacombe, M.; Gill, P. M. W.; Johnson, B.; Chen, W.; Wong, M. W.; Andres, J. L.; Gonzalez, C.; Head-Gordon, M.; Replogle, E. S.; Pople, J. A. *Gaussian 98*, Revision A.11; Gaussian, Inc.: Pittsburgh PA, 2001.

(18) Foresman, J. B.; Frisch, A. In *Exploring Chemistry with Electronic Structure Methods*, 2nd ed.; Gaussian, Inc.: Pittsburgh, PA, 1996.

(19) Arnaud, R.; Subra, R.; Barone, V.; Lelj, F.; Olivella, S.; Solé, A.; Russo, N. *J. Chem. Soc., Perkin Trans. 2* **1986**, 1517–1524.

(20) Pacey, P. D. *J. Chem. Educ.* **1981**, 58, 612–615.

(21) Coote, M. L.; Henry, D. J. *Macromolecules* **2005**, 38, 5774–5779.

(14) Alam, M. M.; Watanabe, A.; Ito, O. *Int. J. Chem. Kinet.* **1996**, 28, 405–411.

(15) Scaiano, J. C. *J. Phys. Chem.* **1981**, 85, 2851–2855.

(16) Lalevée, J.; Allonas, X.; Fouassier, J. P. *Chem. Phys. Lett.* **2005**, 415, 202–205.

**TABLE 2.** Electronic Properties for the Ten Alkenes and Two Radicals Used

	$IP$ (eV) <sup>a</sup>	$EA$ (eV) <sup>a</sup>	$\chi$ (eV) <sup>a</sup>
AN	10.5 (10.9)	0.12 (−0.2)	5.3 (5.4)
MA	9.64 (9.9)	0.09 (−0.5)	4.9 (4.7)
VA	8.91 (9.2)	−0.48 (−1.2)	4.2 (4.0)
VE	8.31 (8.8)	−1.5 (−2.2)	3.4 (3.3)
ABE	8.77	−1.01	3.88
AAM	9.3	−0.11	4.59
NVP	8.06	−0.7	3.68
VC	7.18	0.00	3.6
FU	9.56	1.21	5.38
MAL	9.3	1.00	5.15
<b>I</b>	8.93	3.33	6.13
<b>II</b>	4.96	−0.35	2.31

<sup>a</sup> At UB3LYP/6-31+G\* and ZPE corrected. In parentheses are the experimental data from ref 1.

from eq 1.<sup>22–23</sup> The same procedure was used to obtain the absolute electronegativity ( $\chi_R$ ) of the radicals.

$$\chi = (IP + EA)/2 \quad (1)$$

## Discussion

**The High Reactivity and Low Selectivity of I.** For the monosubstituted alkene monomers, a striking feature is that the  $k_a$  values—which span at least 4 orders of magnitude for **II**—change by less than 1 order for **I** and always remain very high ( $k_a > 10^7 \text{ M}^{-1} \text{ s}^{-1}$ ). **I** appears highly reactive and exhibits a low selectivity. To the best of our knowledge, *there has never been a report of such an enhanced property*. For example, for the phenylthiyl radical and the corresponding derivatives, the reactivity is strongly decreased (the rate constants of addition are found lower by a factor of about 1 000! for the alkenes investigated) and the selectivity is rather high (this structure being mainly reactive with alkenes bearing withdrawing substituents).<sup>11</sup>

For a better understanding of this unusual behavior, quantum mechanical calculations were carried out. The different parameters characterizing the addition process of **I** and **II** to the different alkenes ( $\Delta H_R$ ,  $\delta^{TS}$ , and  $E_a$ ) and the calculated addition rate constants ( $k_a$ ) are presented in Table 3. For the I/VE, I/NVP, I/VC, II/FU, and II/MAL systems, barrierless reactions were found and the TS structure cannot be determined. For these systems, the  $k_a$  values were calculated using the activation entropy determined for I/VA and II/AN (these two reactions also being almost barrierless).

The calculated and experimental  $k_a$  values are compared for **I** and **II** in Figure 1. An excellent general agreement is observed. For **II**, only the limiting values are reported for the addition to VA, VE, ABE, NVP, and VC. The calculated values are found systematically lower than the experimental ones by about 1 order of magnitude. This kind of behavior has been recently observed for other sulfur-centered radicals,<sup>12</sup> and such a difference is known for other systems in the literature.<sup>1,24,25</sup> Keeping in mind the difficulty<sup>18</sup> in acquiring an accurate determination of the transition state structure and knowing that  $k_a$  values span more than 4 order of magnitude, the observed agreement can be

(22) Parr, R. G.; Pearson, R. G. *J. Am. Chem. Soc.* **1983**, *105*, 7512–7516.

(23) Pearson, R. G. *J. Am. Chem. Soc.* **1985**, *107*, 6801–6806.

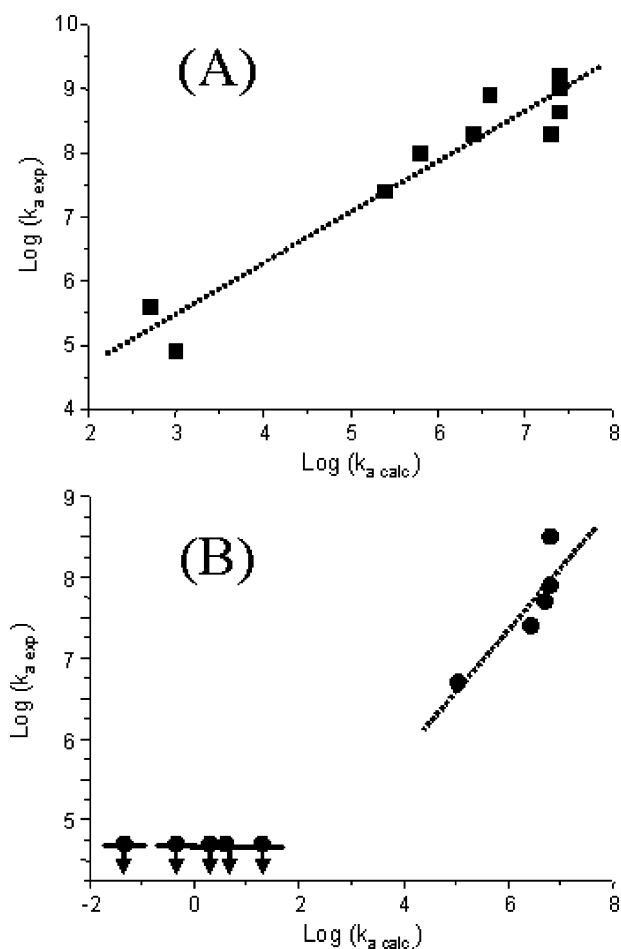
(24) Coote, M. L. *Macromolecules* **2004**, *37*, 5023–5031.

(25) Henry, D. J.; Coote, M. L.; Gomez-Balderas, R.; Radom, L. *J. Am. Chem. Soc.* **2004**, *126*, 1732–1740.

**TABLE 3.** Thermodynamical Data and Transition State Properties for the Different Radical/Alkene Systems (see text)

system	$\Delta H_R^a$ (kJ/mol)	$\delta^{TS,b}$	$d(X-C)$ (Å)	barrier <sup>a</sup> (kJ/mol)	$\log(k_{a,calc})$
I/AN	−30.4	−0.135	2.647	11.5	5.4
I/MA	−25.1	−0.124	2.498	8.72	5.8
I/VA	−12.1	−0.25	2.401	0.2	7.3
I/VE	−23.3	−0.304 <sup>c</sup>		0	7.4
I/ABE	−7.3	−0.223	2.574	2.2	6.4
I/AAM	−26.5	−0.15	2.563	4.5	6.6
I/NVP	−20.02	−0.276 <sup>c</sup>		0	7.4
I/VC	−21.03	−0.312 <sup>c</sup>		0	7.4
I/FU	16.42	−0.06	2.317	25.05	2.7
I/MAL	9.40	−0.12	2.37	23.7	3.0
II/AN	−53.1	0.195	2.553	1.9	6.7
II/MA	−41.1	0.189	2.448	2.0	6.4
II/VA	−29.1	0.124	2.251	36.3	0.6
II/VE	−22.4	0.06	2.297	49.3	−1.3
II/ABE	−24.1	0.109	2.27	40.2	−0.3
II/AA	−48.5	0.177	2.439	7.6	5.0
II/NVP	−29.5	0.08	2.306	40.3	0.3
II/VC	−22.6	0.131	2.323	37.1	1.3
II/FU	−31.2	0.36 <sup>c</sup>		0	6.8
II/MA	−43.0	0.32 <sup>c</sup>		0	6.8

<sup>a</sup> Single points at UB3LYP/6-311++G\*\* level on the geometry determined at 6-31G\* level; ZPE corrected at 6-31G\* level. <sup>b</sup> UB3LYP/6-31G\* and ZPE corrected at 6-31G\* level. <sup>c</sup> Charge transfer for  $d(X-C)$  constrained to 2.4 Å for **I** and 2.5 Å for **II**.

**FIGURE 1.** Plot of  $\log(k_{a,exp})$  vs  $\log(k_{a,calc})$  for **I** (A) and **II** (B).

considered an excellent (Figure 1) reproduction of the evolution trend. Determination of accurate calculated values obviously requires the use of more sophisticated quantum calculations.

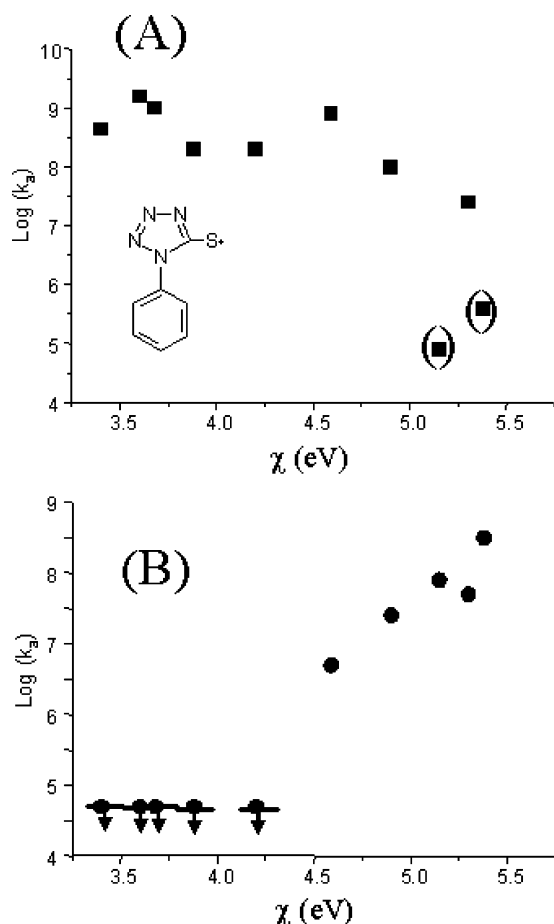


**FIGURE 2.** Plot of  $\log(k_{a,\text{exp}})$  vs  $\chi$  for **I** (A) (the experimental data for bisubstituted monomers MAL and FU are given in brackets) and **II** (B).

For **I**, the experimental equilibrium constants of  $K$  for the addition/fragmentation process correlate with the addition reaction exothermicity ( $\ln(K) = 0.424 - 0.107 \Delta H_R$  ( $r = 0.86$ )). The same effect observed in mercaptobenzoxazoles<sup>12</sup> was ascribed to the large influence of  $\Delta H_R$  on  $k_{-a}$ . A more detailed analysis of the factor governing  $k_{-a}$  is beyond the scope of this paper.

The electron acceptor properties of the different alkenes decrease with the absolute electronegativity in the series  $\text{FU} > \text{AN} > \text{MAL} > \text{MA} > \text{AAM} > \text{VA} > \text{ABE} > \text{NVP} > \text{VC} > \text{VE}$  (Table 2). The  $k_a$  change with the monomer electronegativity is depicted in Figure 2.

The behavior of **I** is particularly worthwhile. The remarkable low selectivity toward the addition process is still outlined for the complete range of monomer electronegativity going from the electron-rich  $\pi$ -system (VE, NVP, VC, ...) to the electron-deficient alkenes (AN, MA, AAM, ...), except for the two bisubstituted alkene monomers FU and MAL. In the latter case, the steric hindrance destabilizes the adduct radical: the reaction is less exothermic than expected from the electronegativity values. Comparatively, the carbon-centered structure **II** is found to be rather selective with an enhanced reactivity toward electron-deficient alkenes (particularly for monomer exhibiting  $\chi > 4.5$  eV) and a very low reactivity toward electron-rich structures ( $k_a \ll 5 \times 10^4 \text{ M}^{-1} \text{ s}^{-1}$ ). The behavior of **I** probably corresponds to a unique feature. This behavior can be worthwhile for synthesis applications including C–S single bond

formation. Through such an analysis of **I** reactivity, the proposition of new efficient sulfur-centered structures will be possible in forthcoming studies.

The charge transfers observed for the different radical/alkene systems are presented in Table 3. For **I**,  $\delta^{\text{TS}}$  is always found to be negative, indicating its electrophilic character. **II** appears to be nucleophilic with a net charge transfer from the radical to the alkene for all of the monomers studied. These behaviors are also reflected, as expected, by the radical electronegativity ( $\chi_R$ ) as the absolute electronegativity difference (radical/alkene) and the driving factor for the charge transfer.<sup>6,22,23</sup> For  $\chi_R > \chi_M$ , charge transfer is observed from the alkene to the radical and for  $\chi_R < \chi_M$ , from the radical to the alkene. Interestingly, clear relationships are found between  $\delta^{\text{TS}}$  and  $\chi$ . For **I**, this transfer (in absolute value) increases from AN to VE ( $\delta^{\text{TS}} = -0.692 + 0.112\chi_M$  ( $r = 0.96$ )). For **II**, an opposite trend is observed:  $\delta^{\text{TS}}$  increases from VE to AN ( $\delta^{\text{TS}} = -0.296 + 0.107\chi_M$  ( $r = 0.86$ )).

**TS Structures.** The distances determined by quantum mechanical calculations in the TS between the radical center (carbon or sulfur atom) and the attacked carbon of the double bond  $d(\text{X}-\text{C})$  are presented in Table 3. For **I** and **II**, the bond formation in the TS structure correlates with  $\Delta H_R$  (for **I**,  $d(\text{X}-\text{C}) = 2.421 - 0.0056\Delta H_R$ ; for **II**,  $d(\text{X}-\text{C}) = 2.093 - 0.0080\Delta H_R$ ), in agreement with Hammond's postulate, which states that the placement of a transition structure is directly related to reaction exothermicity. Interestingly, the points concerning **II** are still clearly beyond the correlation obtained for **I**; i.e., the structures of the corresponding TS's are earlier for **I** than for **II**. The  $d(\text{X}-\text{C})$  shift between these compounds is about 0.25 Å: for an exothermicity of 25 kJ/mol,  $d(\text{C}-\text{C})$  is about 2.25 Å for **II** and about 2.50 Å for **I**.

**Polar and Enthalpy Contributions for C• and S•.** From the SCD approach, the barrier is affected by the reaction exothermicity and the participation of a charge transfer in the TS. The polar effect ( $\Delta E_{\text{pol}}$ ) is proportional to  $(\delta^{\text{TS}})^2$ .<sup>22,23</sup> Therefore, a multiple regression analysis of the dependence of  $E_a^{\text{TS}}$  vs  $\Delta H_R$  and  $(\delta^{\text{TS}})^2$  can be obtained for **I** (eq 2) and **II** (eq 3) using the Origin 7.5 software<sup>26</sup> (obviously, the barrierless reactions were not included in the analysis).

$$E_a = 22.8 + 0.30\Delta H_R - 326.5(\delta^{\text{TS}})^2 \quad r^2 = 0.90 \quad (2)$$

$$E_a = 63.9 + 0.45\Delta H_R - 1010(\delta^{\text{TS}})^2 \quad r^2 = 0.98 \quad (3)$$

Equation 3 is close to the expression derived for many C•/alkene couples:<sup>6</sup>  $E_a = 64.9 + 0.41\Delta H_R - 775(\delta^{\text{TS}})^2$ . These two equations underline this important difference between carbon- and sulfur-centered radicals.

From eqs 2 and 3 ( $E_a = E_0 + \alpha\Delta H_R + \beta(\delta^{\text{TS}})^2$ ), we have an access to  $E_0$  (called hereafter the intrinsic barrier) which represents the barrier for  $\Delta H_R = 0$  without any polar effects. This term is about 3 times lower for **I** than for **II**. This is clearly a new point.

The second term in these equations ( $\alpha$ ) describes the enthalpy and basically represents the Evans–Polanyi relationship which

(26) Origin 7.5; OriginLab Corporation: Northampton, MA, 2003.

(27) Semenov, N. N. *Some Problems in Chemical Kinetics and Reactivity*; Princeton Press: Princeton, NJ, 1958.

(28) Lalevée, J.; Allonas, X.; Fouassier, J. P. *Chem. Phys. Lett.* **2005**, *415*, 287–290.

states that the barrier decreases when there is an increase in exothermicity.<sup>27</sup> About one-third and one-half of the  $\Delta H_R$  change are transferred to the TS structures for **I** and **II**, respectively. Interestingly, the transfer coefficient ( $\alpha$ ) is lower for **I**. For **II**, the transfer coefficient is in excellent agreement with the value previously found for a large variety of carbon-centered radicals.<sup>6</sup>

All of these behaviors can probably be ascribed to the symmetry and the overlap of the molecular orbitals involved in the TS's, which are different for **I** and **II**. Indeed, in the SCD approach the reaction surface is strongly related to the mixing of the potential energy profiles of the lowest doublet configurations of the R/alkene system. This mixing strongly depends on the orbitals involved.<sup>3,4</sup> Nowadays, a quantification of this factor remains an outstanding problem in quantum chemistry.<sup>3</sup> However, from the different frontier orbitals involved in **I** and **II**, it can be reasonably assumed that this factor influences both  $E_0$  and  $\alpha$ .

The third part ( $\beta$ ) of these equations differs with the Evans–Polanyi approach and takes into account the polar term. For **II**, the coefficient for the polar factor (1 010) is close to that recently found for carbon-centered radicals (775).<sup>6</sup> For **I**, a lower value is noted (326). This is in agreement with the different electronegativity of the sulfur- and carbon-centered structures.

For **I**, the polar and enthalpy factors exhibit antagonist effects from VE to AN. This is not the case for **II**; i.e., both factors increase in this series. Therefore, the barrier change in the VE–AN series is lower for **I**, explaining its lower selectivity. Concomitantly, the associated lower  $E_0$  of **I** will also lead to a higher reactivity (lower  $E_a^{TS}$ ).

## Conclusion

One fascinating aspect of radical **I** should be its ability to initiate the polymerization processes of a large variety of monomers; this cannot be done with any known initiating radicals. From the chemical reactivity point of view, a large panel of radical/double bond situations could be expected through a careful selection of sulfur-centered radicals thereby allowing a further general discussion of the observed properties. The addition of  $S^\bullet$  onto double bonds can also give access to a large variety of C–S single bond formations.

**Acknowledgment.** The authors thank the CINES (Centre Informatique National de l'Enseignement Supérieur) for the generous allocation of time on the IBM SPsupercomputer.

JO061793W